Journal of Evolutionary Biology, 2024, **37**, 14–27
https://doi.org/10.1093/jeb/voad008
Advance access publication 11 December 2023
Research Article

JOURNAL OF
Evolutionary Biology

eseb
European Society for Evolutionary Biology

Microgeographic speciation in a complex of Anatolian bush crickets facilitated by fast evolution of reproductive isolation

Joaquín Ortego[1], Sarp Kaya[2], Battal Çıplak[3], L. Lacey Knowles[4]

[1]Department of Ecology and Evolution, Estación Biológica de Doñana, EBD-CSIC, Seville, Spain
[2]Health Services, Vocational Schools, Mehmet Akif Ersoy University, Burdur, Turkey
[3]Department of Biology, Faculty of Science, Akdeniz University, Antalya, Turkey
[4]Department of Ecology and Evolutionary Biology, University of Michigan, Ann Arbor, MI, United States

Corresponding author: Joaquín Ortego, Department of Ecology and Evolution, Estación Biológica de Doñana, EBD-CSIC, Avda. Américo Vespucio 26, E-41092 Seville, Spain. Email: joaquin.ortego@csic.es

Abstract

Identifying the drivers of microgeographic speciation (i.e., speciation over small, local geographic scales) is key to understand the origin of speciose groups. Here, we use genomic data to infer the demographic processes underlying diversification in *Poecilimon luschani* (Orthoptera: Tettigoniidae), a species complex belonging to the most diverse genus of bush crickets from the Mediterranean region (>170 taxa) that comprises three recognized subspecies with small allopatric distributions in the topographically complex Teke Peninsula, southwestern Anatolia. Phylogenomic reconstructions that include all other taxa within the species group confirmed that subspecies of *P. luschani* originated from a common ancestor during the Pleistocene, supporting recent (<1 Ma) diversification within a small geographical area (ca. 120 × 80 km). Genetic clustering analyses corroborated the distinctiveness of each subspecies and the cohesiveness of their respective populations, with abrupt genetic discontinuities coinciding with contemporary range boundaries. Indeed, our analyses uncovered the presence of two sympatric cryptic sister lineages that diverged <300 ka ago and do not admix despite being co-distributed. Collectively, these results support that all lineages within the complex represent independently evolving entities corresponding to full-fledged species. Statistical evaluation of alternative models of speciation strongly supports a scenario of divergence in isolation followed by a period of limited gene flow during the last glacial period, when all lineages experienced marked expansions according to demographic reconstructions. Our study exemplifies how localized allopatric divergence and fast evolution of reproductive isolation can promote microgeographic speciation and explain the high rates of endemism characterizing biodiversity hotspots.

Keywords: allopatric speciation, cryptic diversity, evolution of reproductive isolation, Mediterranean biodiversity hotspot, microgeographic speciation

Introduction

Biodiversity hotspots have been hypothesized to originate from the accumulation of species over extended periods of time prompted by environmental stability and slow extinction rates (i.e., evolutionary "museums" hypothesis), as a consequence of high rates of speciation (i.e., "cradles" for biological diversity hypothesis), or through the co-occurrence of both phenomena (Stebbins, 1974; e.g., Moreau & Bell, 2013; Tzedakis, 2009). Determining the microevolutionary processes underlying such macroevolutionary patterns of biological diversity is of paramount importance to elucidate the origin of species richness gradients and understand why some regions host an extraordinary number of species compared with others (Li et al., 2018; Singhal et al., 2022).

Microendemic species—taxa with restricted geographical distributions—from highly diverse groups often contribute disproportionally to species richness in biodiversity hotspots (e.g., Madagascar: Wilmé et al., 2006; New Caledonia: Bradford & Jaffre, 2004; Cape Region: Goldblatt & Manning, 2002), yet our understanding on their origins is still tremendously limited (Bradford & Jaffre, 2004; Cowling & Pressey, 2001). Although palaeoecological evidence indicates that several species with narrow distributions have a geographical relict origin (i.e., resulted from range contraction of a formerly more widespread taxon; Grandcolas et al., 2014), high rates of microendemism in hyperdiverse evolutionary radiations are likely to have originated via in situ speciation at small spatial scales (Goldblatt & Manning, 2002; Musher et al., 2022). Different mechanisms have been proposed to explain microgeographic diversification, including sympatric/ecological speciation (Papadopulos et al., 2011), parapatric/peripatric divergence favoured by reduced gene flow across strong selection differentials (Anacker & Strauss, 2014; Goldblatt & Manning, 2002; Levin, 1993), or allopatric speciation during periods of isolation in climatic microrefugia (Musher et al., 2022). Fine-scale landscape heterogeneity and complex mosaics of contrasting environments (i.e., potential for local adaptation), high topographic complexity (i.e., potential for isolation), and environmental stability (i.e., opportunity for lineage persistence) offer an ideal biogeographic arena for small-scale speciation to occur and newly generated lineages persist through evolutionary time (Bradford & Jaffre, 2004; Goldblatt & Manning, 2002; Wilmé et al., 2006).

Received March 22, 2023; revised October 9, 2023; accepted November 13, 2023

The Mediterranean biodiversity hotspot, extending from the Macaronesian archipelagos to the Middle East, is the second largest biodiversity hotspot in the world and the third in terms of plant diversity (Myers et al., 2000; Medail & Quezel, 1997). A considerable number of narrowly distributed taxa that are locally endemic (e.g., >25,000 plant species of which >50% are endemic; Nieto Feliner, 2014) contribute to the outstanding levels of species diversity of the region compared with surrounding areas. Different geologic and climatic factors have been proposed to explain such extraordinary levels of biodiversity and local endemism, including the high topographic complexity of the region, the connectivity and isolation of different landmasses due to sea-level changes linked to the Messinian Salinity Crisis (ca. 5.96–5.33 Ma) and glacio-eustatic fluctuations (ca. 2.59–0.02 Ma), and the limited impact of Quaternary climatic oscillations compared with higher latitudes (Nieto Feliner, 2014; Tzedakis, 2009; e.g., Noguerales et al., 2021; Ortego et al., 2022). These factors have likely promoted population isolation and allopatric divergence (e.g., in glacial–interglacial microrefugia; Gómez & Lunt, 2007) and provided the opportunity for ecological speciation across steep environmental gradients (e.g., Steinbauer et al., 2013). Moreover, topographic complexity and landscape heterogeneity contribute to newly generated lineage persistence to changing environmental conditions with small-scale range shifts, reducing extinction rates, and allowing the progressive accumulation of diversity over time (Nieto Feliner, 2011; Tzedakis, 2009). Identifying the proximate drivers of microgeographic speciation and distinguishing among alternative evolutionary scenarios is crucial for understanding the origin of narrow endemic taxa and establishing strategies aimed at preserving not only species but also the ecological and evolutionary processes that generate and sustain such diversity (Cowling & Pressey, 2001; Moritz, 2002).

With 146 species and 42 subspecies organized in two subgenera and 17 species groups, *Poecilimon* (Orthoptera: Tettigoniidae) constitutes the most diverse genus of bush crickets in the Western Palaearctic and includes a high number of narrowly distributed taxa (Cigliano et al., 2023; Çıplak, 2003; for a recent revision of the genus, see Borissov et al., 2023). Most taxa are distributed in Anatolia, Aegean, and Ponto-Caspian regions, encompassing the Mediterranean, Irano-Anatolian, and Caucasus biodiversity hotspots (Borissov et al., 2023; Cigliano et al., 2023). Subtle diagnostic characters have contributed to considerable taxonomic uncertainty within the genus, with a continuous description of new species and frequent taxonomic reassessments (e.g., Borissov et al., 2023; Boztepe et al., 2013; Kaya et al., 2015). The low dispersal capacity of *Poecilimon*—all taxa are flightless—together with its complex acoustic behaviour (Borissov et al., 2023) have likely contributed to population fragmentation and quick evolution of reproductive isolation (e.g., prezygotic barriers to gene flow), respectively. These attributes make the genus *Poecilimon* an excellent candidate model system to study the proximate processes underlying diversification over small geographic scales (Borissov et al., 2023; Boztepe et al., 2013; Kaya et al., 2015). Here, we employ genomic data to infer the demographic processes underlying microgeographic diversification in *Poecilimon* (*Poecilimon*) *luschani* Ramme, 1933, a complex that currently comprises three subspecies (*P. l. luschani* Ramme, 1933, *P. l. chobanovi* Boztepe, Kaya & Çıplak, 2013, and *P. l. birandi* Karabag, 1950) that were described on the basis of subtle differences in the shape of male cerci and have narrow distributions in Teke Peninsula, southwestern Anatolia (Boztepe et al., 2013). Although the three putative subspecies are allopatric, they present adjacent distributions and occupy a wide variety of open habitats (e.g., maquis, forest clearings, and shrublands) and elevational ranges, from sea level to alpine zones in the Western Taurus mountains (>2,000 m; Figures 1 and 2; Boztepe et al., 2013; Kaya et al., 2015). This suggests that eco-environmental specialization within the complex is limited and that the

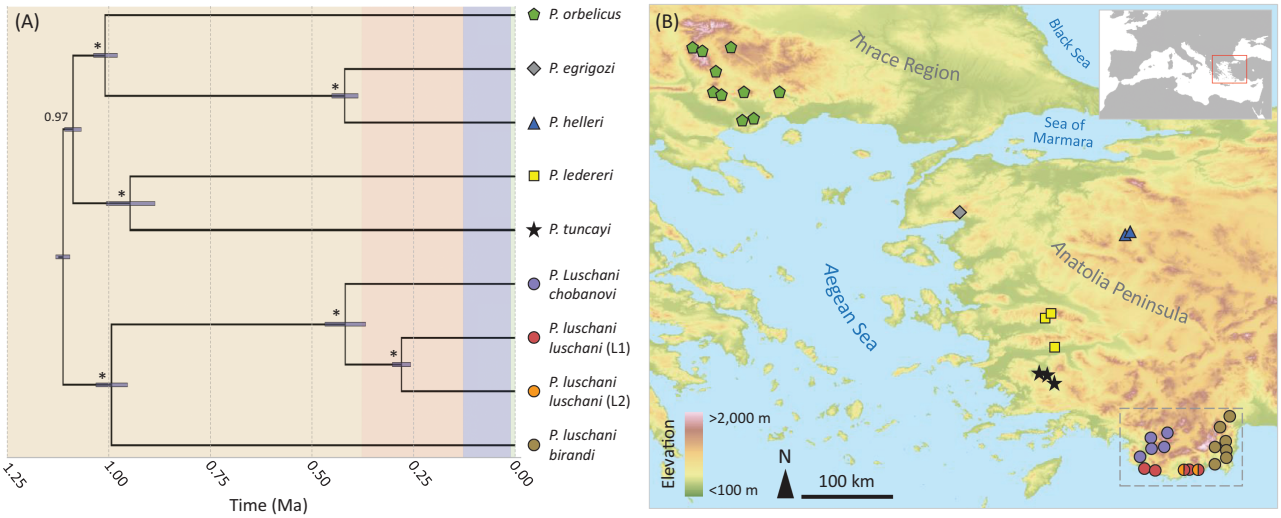

Figure 1. (A) Phylogenetic relationships among taxa comprising the species group *Poecilimon luschani* and (B) map showing their respective geographic distributions in Anatolia and Thrace regions based on available occurrence records. Phylogenetic relationships (option A01) and divergence times (option A00) were estimated using BPP (3,414 loci). Numbers on nodes are posterior probability (PP) support values (* = 1), and bars show 95% highest posterior densities (HPD) of divergence time estimates assuming a genomic mutation rate of 2.8×10^{-9} per site per generation and a 1-year generation time. The root position was estimated by BPP along with the other nodes of the tree. Background colours indicate geological divisions of the Quaternary (yellow: early Pleistocene; red: middle Pleistocene; blue: late Pleistocene; green: Holocene). Phylogenetic analyses were run considering as independent lineages the three currently recognized subspecies (*P. l. chobanovi*, *P. l. luschani*, and *P. l. birandi*) and the two sympatric cryptic lineages (L1 and L2) of *P. luschani*. Dashed area on map is shown enlarged in Figure 2.

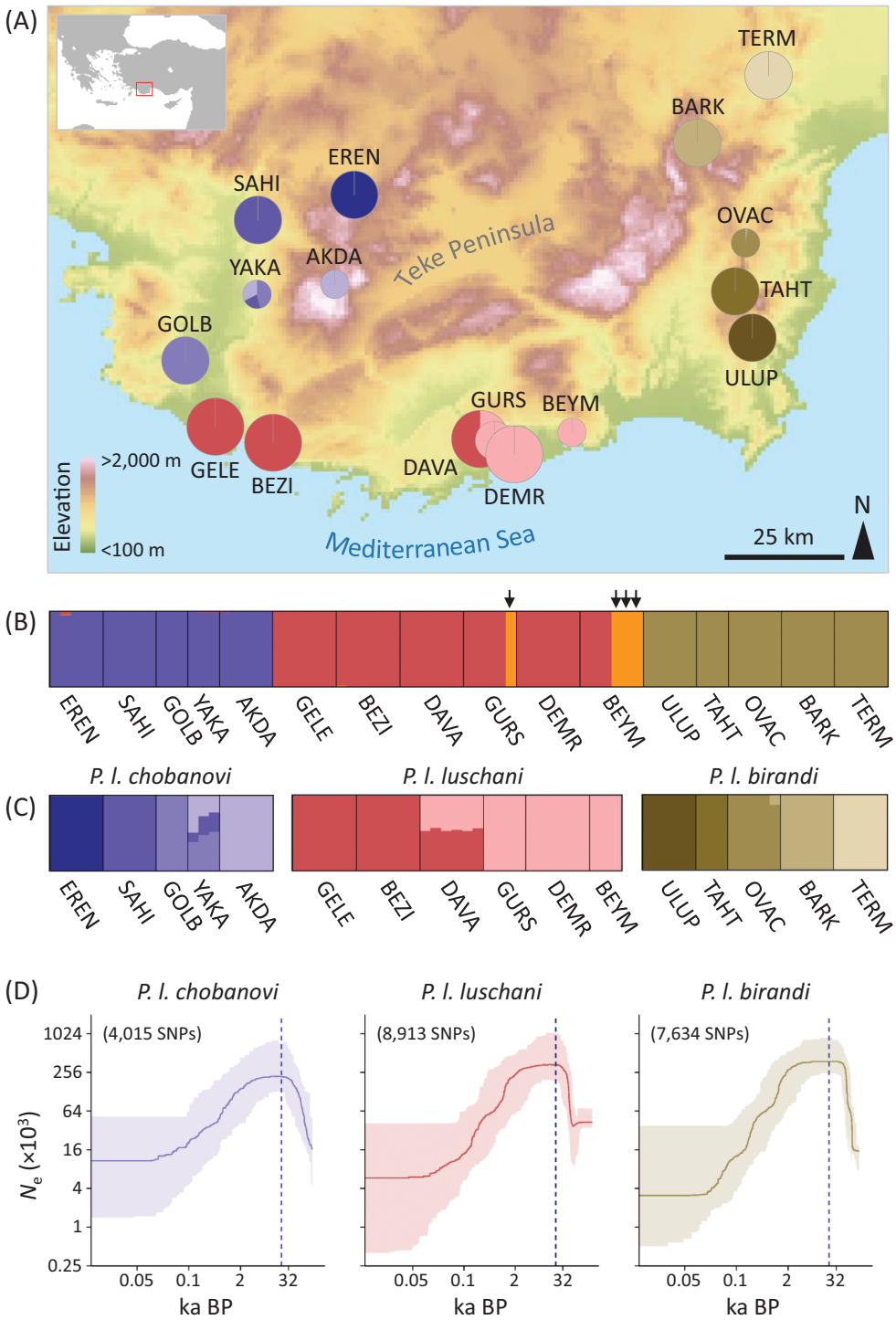

Figure 2. (A–C) Results of genetic assignments based on STRUCTURE and (D) demographic reconstructions inferred using STAIRWAY PLOT for the three currently recognized subspecies within the taxon *Poecilimon luschani*. Hierarchical STRUCTURE analyses were run for (B) all populations of the three subspecies jointly (6,611 SNPs) and (C) independently for populations of each subspecies (*P. l. chobanovi*: 10,419 SNPs; *P. l. luschani*: 18,392 SNPs; *P. l. birandi*: 17,369 SNPs). Pie charts on map (A) show the geographic location of analysed populations and their respective genetic assignments. In barplots (B, C), each individual is represented by a vertical bar partitioned into *K* coloured segments showing the individual's probability of belonging to the cluster with that colour; thin vertical black lines separate individuals from different populations. Results of STRUCTURE for each dataset are shown for the value of *K* at which the log probability of the data (LnPr(X|*K*)) reached a plateau (see Supplementary Figure S3). Results from $K = 2$ to $K = 5$ are presented in Supplementary Figure S4. STAIRWAY PLOT graphs (D) show the median (solid lines) and 2.5 and 97.5 percentiles (shaded areas) of effective population size (N_e) through time, estimated assuming a genomic mutation rate of 2.8×10^{-9} per site per generation and a 1-year generation time (both axes in a logarithmic scale); vertical dashed lines indicate the Last Glacial Maximum (LGM; ca. 21 ka) and number of polymorphic SNPs used to calculate the site frequency spectrum (SFS) in parentheses. STRUCTURE (C) and STAIRWAY PLOT (D) analyses for the subspecies of *P. l. luschani* were run excluding lineage L2, which was only found in two localities and four individuals (arrows in B). Population codes as described in Table 1.

different putative taxa have likely diverged in allopatry (Boztepe et al., 2013). Preliminary mtDNA-based studies did not find support for the monophyly of the three subspecific taxa, which points to incomplete lineage sorting and/or historical introgression and raises doubts about their taxonomic status (Boztepe et al., 2013; Kaya et al., 2015). The contemporary allopatric distribution of most taxa within the genus *Poecilimon*, together with their subtle phenotypic and ecological differentiation, exemplifies the longstanding difficulty of establishing and testing taxonomic hypotheses when reproductive isolation among candidate species cannot be measured in contact zones (Coyne & Orr, 2004; Mayr, 1963). Under such a scenario, a comprehensive taxonomic and population sampling, time-calibrated phylogenetic reconstructions, and testing of alternative demographic scenarios can help to estimate the minimum time of divergence for strong reproductive isolation to evolve (i.e., a proxy for reproductive isolation and speciation time) and provide a baseline for species delimitation among currently allopatric taxa (Coyne & Orr, 1989; Dynesius & Jansson, 2014).

Using as a model system the complex *P. luschani*, we aim to better understand the demographic processes underlying microevolutionary speciation and gain insights into the origin of the high rates of local endemism that characterizes the Mediterranean biodiversity hotspot. Specifically, we (a) first reconstructed the phylogenetic relationships among all taxa within the focal species group and estimated the timing of diversification. These analyses corroborated the Pleistocene origin of the group and the geographic dimension of speciation, pointing to the interplay between Quaternary climatic oscillations and the complex topography of the region in promoting population fragmentation and allopatric divergence. Second, we (b) analysed range-wide populations of each putative taxon within *P. luschani* to evaluate the genetic cohesiveness across their respective populations and determine whether their range limits coincide with abrupt genetic discontinuities, as would be expected for independently evolving entities (i.e., full-fledged species), or whether they show clinal transitions characteristic of non-reproductively isolated lineages (i.e., conspecific populations or subspecies). Different lines of evidence supported the evolutionary and taxonomic distinctiveness of all lineages recovered by our genomic analyses, indicating that they represent full-fledged species. Provided this, (c) we applied a model-based approach to evaluate alternative scenarios of divergence and gene flow and gain insights into the demographic processes underlying microgeographic speciation. Considering the close geographical proximity of the focal taxa and, thus, ample opportunity for secondary contact during periods of demographic expansions, a total lack of post-divergence gene flow would be indicative of short speciation times and fast evolution of total reproductive isolation. Alternatively, evidence for historical gene flow during phases of demographic expansions would be compatible with semi-permeable species boundaries and a more progressive accumulation of reproductive isolation, suggesting that lineages have persisted through evolutionary time despite episodes of secondary contact and introgression.

Materials and methods

Population and taxonomic sampling

We sampled populations covering the known distributional range of each of the three recognized subspecies within the taxon *Poecilimon* (*Poecilimon*) *luschani* Ramme, 1933: *Poecilimon* (*Poecilimon*) *luschani luschani* Ramme, 1933, *Poecilimon* (*Poecilimon*) *luschani chobanovi* Boztepe, Kaya & Çıplak, 2013, and *Poecilimon* (*Poecilimon*) *luschani birandi* Karabag, 1950 (Boztepe et al., 2013; Cigliano et al., 2023; Table 1). For phylogenomic analyses (see section Phylogenomic inference and divergence time estimation), we also obtained samples from representative populations of each of the five other taxa comprising the species group *P.* (*Poecilimon*) *luschani* Ramme, 1933 (Boztepe et al., 2013; Cigliano et al., 2023; Table 1). Note that the taxonomy of the genus *Poecilimon* is constantly changing (Cigliano et al., 2023; e.g., Borissov et al., 2023; Boztepe et al., 2013). For the sake of this study, we refer to the species group *P. luschani*, which itself remains monophyletic according to available phylogenetic evidence on the genus, despite the proposed merger of the species group *P. luschani* into the larger species group *Poecilimon* (*Poecilimon*) *ampliatus* Brunner von Wattenwyl, 1878 (Borissov et al., 2023). Sampling was designed using our own species occurrence data and records available in the literature (Boztepe et al., 2013; Kaya et al., 2012, 2015), Orthoptera Species File (http://orthoptera.speciesfile.org/; Cigliano et al., 2023), and the Global Biodiversity Information Facility (GBIF.org, 29 October 2022, GBIF Occurrence Download https://doi.org/10.15468/dl.mkvf78) (Figure 1). We recorded spatial coordinates using a GPS and preserved samples in 96% ethanol at −20 °C until needed for genomic analyses. Specimens are deposited at Akdeniz University, Department of Biology, Zoological Museum, Antalya, Türkey (AUZM). Further details on sampling locations are provided in Table 1.

Genomic library preparation and processing

We processed genomic DNA into one genomic library using the double-digestion restriction-site-associated DNA sequencing procedure (Peterson et al., 2012), as detailed in Supplementary Methods S1. Raw sequences were demultiplexed and preprocessed using STACKS v. 1.35 (Catchen et al., 2013) and assembled with PYRAD v. 3.0.66 (Eaton, 2014); see Supplementary Methods S2 for details on assembling and filtering of sequence data. Note that the choice of different filtering and assembling thresholds had a little impact on the obtained inferences (e.g., Eaton, 2014; González-Serna et al., 2018; Ortego et al., 2018). For this reason, unless otherwise indicated, all downstream analyses were performed using datasets of unlinked single-nucleotide polymorphism (SNPs) (i.e., using a single random SNP per RAD locus, including singletons), obtained with PYRAD considering a clustering threshold of sequence similarity of 85% ($W_{clust} = 0.85$) and discarding loci that were not present in at least 50% of individuals (*minCov* = 0.50).

Phylogenomic inference and divergence time estimation

We used the multispecies coalescent model implemented in the program BPP v. 4.1 (Flouri et al., 2018) to (a) reconstruct the phylogenetic relationships among taxa/lineages (analysis A01) and (b) estimate divergence times (analysis A00). The *.loci* file from PYRAD was edited and converted into a BPP input file using custom R scripts written by J.-P. Huang (https://github.com/airbugs/; for details, see Huang et al., 2020). Briefly, we trimmed all loci to 110 bp and excluded those that were not represented in at least one individual per lineage (i.e., loci with missing lineages were removed). Due to

Table 1. Geographical location of sampling sites for taxa comprising the species group *Poecilimon luschani*, including the range-wide studied populations of the three recognized subspecies within the taxon *P. luschani*. The two sympatric cryptic lineages (L1 and L2) identified on the basis of genomic data within the taxon *P. l. luschani* are also indicated.

Species	Locality	Code	Latitude	Longitude	Elevation	*n*
P. orbelicus	Pirin Mt.	PIRI	41.80446	23.46846	1,280	3
P. egrigozi	Samrık	SAMR	39.40281	29.14619	1,680	3
P. helleri	Beyoba Mahallesi	BEYO	39.70032	26.87033	1,700	3
P. ledereri	Bozdağ	BOZD	38.34765	28.10867	1,520	3
P. tuncayi	Eskiçine	ESKI	37.53187	28.04837	80	3
P. luschani chobanovi	Erentepe Mt.	EREN	36.74397	29.64583	2,020	5
	Sahilceylan	SAHI	36.70044	29.41639	770	5
	Gölbent	GOLB	36.42597	29.27336	110	3
	Yakaköy	YAKA	36.55817	29.42150	440	3
	Akdağ Mt.	AKDA	36.57731	29.58311	2,280	5
P. luschani luschani (L1)	Gelemiş	GELE	36.28958	29.33431	90	6
	Bezirgan	BEZI	36.26214	29.46531	840	6
	Davazlar	DAVA	36.25952	29.87975	550	6
	Gürses	GURS	36.26570	29.92766	550	4
	Demre	DEMR	36.24470	29.94612	150	6
	Beymelek Lagünü	BEYM	36.27576	30.05586	10	3
P. luschani luschani (L2)	Gürses	GURS	36.26570	29.92766	550	1
	Beymelek Lagünü	BEYM	36.27576	30.05586	10	3
P. luschani birandi	Ulupınar	ULUP	36.45144	30.42819	320	5
	Tahtalı Dağı Mt.	TAHT	36.54678	30.40988	1,610	3
	Ovacık	OVAC	36.65976	30.41469	1,150	5
	Bakirlidăg Mt.	BARK	36.84297	30.32055	2,020	5
	Termesos	TERM	36.98583	30.46562	950	5

Note. *n* = number of genotyped individuals.

large computational demands, we only included in the analyses three representative individuals for *P. luschani chobanovi*, *P. luschani birandi*, and each of the two sympatric lineages (hereafter, L1 and L2) identified by genetic clustering analyses within the subspecies *P. luschani luschani* (see section Genetic structure within the complex *P. luschani*). For tree inference analyses (analysis A01), we set uniform rooted trees as species tree prior, applied an automatic adjustment of fine-tune parameters, set the diploid option to indicate that the input sequences are unphased, and adjusted the inverse-gamma distributions of θ (α = 3, β = 0.04) and τ (α = 3, β = 0.07) priors according to empirical estimates calculated from the number of segregating sites per site (Huang et al., 2020). BPP analyses do not require defining an outgroup, as the program samples the root position along with the other nodes of the tree. We ran two independent replicate analyses for 200,000 generations, sampling every 2 generations, after a burn-in of 10,000 generations. To estimate the posterior distribution of divergence times (τ; analysis A01), we ran the analyses using the same dataset and settings described above for tree inference analyses, with two independent replicates for 1,000,000 generations, sampled every 2 generations, after a burn-in of 100,000 generations. We estimated divergence times using the equation $\tau = 2\mu t$, where τ is the divergence in substitutions per site estimated by BPP, μ is the per-site mutation rate per generation, and t is the absolute divergence time in years (Huang et al., 2020). We considered the mutation rate per site per generation of 2.8×10^{-9} estimated for *Drosophila melanogaster* (Keightley et al., 2014), which is similar to the spontaneous mutation rate estimated for the butterfly *Heliconius melpomene* (2.9×10^{-9}; Keightley et al., 2015).

Genetic structure within the complex *P. luschani*

We used the Bayesian Markov chain Monte Carlo clustering method implemented in the program STRUCTURE v. 2.3.3 (Pritchard et al., 2000) to quantify the genetic structure and admixture across the genotyped populations of the three recognized subspecies within the taxon *P. luschani* (Table 1). As recommended by Janes et al. (2017), we conducted STRUCTURE analyses hierarchically, reported the results for multiple values of *K*, and used two statistics to interpret the number of genetic clusters (*K*) that best describe our data at each hierarchical level: log probabilities of Pr(X|*K*) (Pritchard et al., 2000) and ΔK (Evanno et al., 2005). To fully explore population subdivision, we initially analysed the data from all taxa and populations jointly and, subsequently, we ran independent analyses for subsets of populations assigned to the same genetic cluster in the previous hierarchical-level analysis (Janes et al., 2017; e.g., Massatti & Knowles, 2014). We ran STRUCTURE analyses assuming correlated allele frequencies and admixture and without using prior population information. We conducted 15 independent runs for each value of *K* (from *K* = 1 to *K* = 10) to estimate the most likely number of genetic clusters with 200,000 Markov chain Monte Carlo cycles, following a burn-in step of 100,000 iterations. We retained the 10 runs having the highest likelihood for each value of *K*. Complementarily, we performed principal component analyses (PCAs) as implemented in the R v. 4.2.1

(R Core Team, 2023) package "adegenet" (Jombart, 2008). Before running PCAs, we replaced missing data with the mean allele frequency of the corresponding locus estimated across all samples (Jombart, 2008). Finally, we ran SVDQUARTETS as implemented in PAUP* version 4.0a169 (Swofford, 2002) to estimate the relationships among populations from each lineage (i.e., a population/species tree). We used *P. tuncayi* as an outgroup, evaluated 100,000 random quartets from the data set, and quantified uncertainty in relationships using 100 bootstrapping replicates.

Landscape genetic analyses

We tested whether genetic differentiation (F_{ST}) between populations was correlated with (a) geographical and/or (b) weighted topographic distances, given the topographic complexity of the region. Genetic differentiation between populations was calculated in ARLEQUIN v. 3.5 (Excoffier & Lischer, 2010). We used the R package "topodistance" to calculate geographical and weighted topographic distances (Wang, 2020). Weighted topographic distances were calculated using the elevation layer available in WORLDCLIM (https://www.worldclim.org/) and the *topoWeightedDist* function, with a linear function to weight the angle of aspect changes and an exponential function to weight the slope between cells, as recommended by Wang (2020). The correlation between genetic and geographical/topographic distance matrices was analysed using Mantel tests considering all populations from the three putative subspecies (excluding the sympatric, cryptic lineage L2 from *P. l. luschani*). A Mantel test procedure adjusted for incomplete matrices was applied to separate analyses of pairwise comparisons within and across subspecies. Mantel tests were run using ZT software with 10,000 permutations (Bonnet & Van de Peer, 2002).

Testing alternative models of divergence

We used the coalescent-based approach implemented in FASTSIMCOAL2 (Excoffier et al., 2013) to test alternative models of divergence among the three putative subspecies of *P. luschani*: *P. l. chobanovi*, *P. l. luschani*, and *P. l. birandi*. As the different genotyped populations of each taxon exhibited strong genetic cohesiveness and grouped together in STRUCTURE, PCA, and SVDQUARTETS analyses (see section Genetic structure within the complex *P. luschani*), all individuals from each subspecies were pooled for FASTSIMCOAL2 simulations. However, we excluded from the analyses the sympatric, cryptic lineage L2 from the subspecies *P. l. luschani* given the very limited number of individuals in this lineage (see section Genetic structure within the complex *P. luschani*). Considering that contemporary populations of the three putative subspecies are entirely allopatric and genetic clustering analyses do not show any evidence of genetic admixture or ongoing hybridization among them (see section Genetic structure within the complex *P. luschani*), we tested scenarios that considered either total lack of post-divergence gene flow or historical post-divergence gene flow during hypothetical periods of secondary contact (e.g., linked to range expansions). Specifically, we tested models of (a) divergence in strict isolation (Model A), (b) divergence in strict isolation followed by secondary contact and post-divergence gene flow during a limited period of time (Model B), and (c) isolation-with-migration followed by interruption of gene flow (Model C) (Supplementary Figure S1). The last two models consider alternative gene flow scenarios involving different contemporary (i.e., subspecies of *P. luschani*) and/or ancestral populations (Supplementary Figure S1). Note that the lower limit of the timing of interruption of gene flow (T_{GF2} in Model B and T_{ISO} in Model C; see Supplementary Figure S1) is not bounded in our simulations; thus, gene flow (m) under both scenarios can virtually take place until present day (Supplementary Figure S1). For details on FASTSIMCOAL2 analyses and model selection, see Supplementary Methods S3.

Inference of past demographic history

We reconstructed the past demographic history from each putative subspecies of *P. luschani* using the program STAIRWAY PLOT v. 2.1, which implements a flexible multi-epoch demographic model based on the site frequency spectrum that does not require whole-genome sequence data or reference genome information (Liu & Fu, 2020). We computed the site frequency spectrum for each subspecies as described for FASTSIMCOAL2 analyses (Supplementary Methods S3) and ran STAIRWAY PLOT considering the 1-year generation time of *Poecilimon* (Borissov et al., 2023), assuming a mutation rate of 2.8×10^{-9} per site per generation (Keightley et al., 2014), and performing 200 bootstrap replicates to estimate 95% confidence intervals.

Results

Genomic data

The average number of reads retained per individual after the different quality filtering steps was 2,687,804 (range = 887,695–5,228,934 reads; Supplementary Figure S2). On average, this represented 80% (range = 77–82%) of the total number of reads recovered for each individual (Supplementary Figure S2). The final dataset including all populations of *P. luschani* retained 6,611 unlinked SNPs. Datasets for populations of the subspecies *P. l. chobanovi*, *P. l. luschani* (excluding lineage L2), and *P. l. birandi* retained 10,419 SNPs, 18,392 SNPs, and 17,369 SNPs, respectively.

Phylogenomic inference and divergence time estimation

After filtering out loci that were not represented in at least one individual per lineage, the input file for BPP analyses contained 3,414 loci. This represents 22.56% of the 15,131 loci recovered by PYRAD for the dataset including three representative individuals for each lineage (see section Phylogenomic inference and divergence time estimation). Phylogenomic reconstruction in BPP (analysis A01) reveals the presence of two main clades, one comprising the different subspecies/lineages of the taxon *P. luschani* and another that includes the rest of the taxa within the species group (Figure 1A). A subclade including *P. egrigozi* and *P. helleri* from northwestern Anatolia is sister to the Balkan species *P. orbelicus*, the only taxon from the group distributed outside of the Anatolian Peninsula. This subclade is in turn sister to another one including *P. ledereri* and *P. tuncayi*, two taxa with adjacent distributions in southwestern Anatolia. Phylogenomic analyses support the monophyly of the taxon *P. luschani* from Teke Peninsula, with the easternmost taxa *P. l. birandi* being sister to a subclade including *P. l. chobanovi* and the two lineages of *P. l. luschani* (L1 and L2) identified by genetic clustering analyses (see section Genetic structure within the complex *P. luschani*). These two cryptic and partially sympatric lineages of *P. l. luschani* are sister, suggesting that divergence probably

took place within a limited geographical space in southern Teke Peninsula (Figure 1). All nodes are supported with a posterior probability > 0.97 (Figure 1A). BPP analyses (analysis A00) estimate that the two main clades diverged from a common ancestor during the early Pleistocene (ca. 1.08 Ma; Calabrian age; Figure 1A). The divergence of all subclades and species (ca. 0.48–1.08 Ma), as well as the split of the three recognized subspecies within *P. luschani* (ca. 0.42–0.99 Ma), also took place in the early Pleistocene (Figure 1A). Finally, the two cryptic lineages within *P. l. luschani* (L1 and L2) likely diverged in the middle Pleistocene (ca. 0.28 Ma; Chibanian age; Figure 1A).

Genetic structure within the complex *P. luschani*

STRUCTURE analyses including all populations of the three recognized subspecies within the taxon *P. luschani* identify $K = 3$ as the most likely number of clusters according to the ΔK criterion, but LnPr(X|K) reached a plateau at $K = 4$ (Supplementary Figure S3A). For $K = 2$, the two genetic clusters separate *P. l. birandi* from the sister taxa *P. l. chobanovi* and *P. l. luschani* (Supplementary Figure S4A). STRUCTURE analyses for $K = 3$ split populations of the three subspecific taxa, with the exception of four individuals of *P. l. luschani* from localities GURS and BEYM that comprise the L2 cryptic lineage; these individuals show a high admixed ancestry for $K = 3$ but fully separate into a different genetic cluster for $K = 4$ (Figures 2 and 3; Supplementary Figure S4A). STRUCTURE analyses ran independently for the three subspecific taxa reveal marked genetic structure. Analyses for populations of *P. l. chobanovi* identified that the most likely number of clusters is $K = 2$ according to the ΔK criterion, but LnPr(X|K) reached a plateau at $K = 4$ (Supplementary Figure S3C). All populations split hierarchically into different genetic clusters from $K = 2$ to $K = 4$ with no signatures of genetic admixture, except population YAKA (Figures 2 and 3; Supplementary Figure S4B); this population is located in the centre of the taxon's distribution and presents a considerable degree of admixed ancestry from different genetic clusters for $K = 3$–4 (Figures 2 and 3; Supplementary Figure S4B). STRUCTURE analyses focused on populations of *P. l. luschani* (excluding the cryptic lineage L2) identify that the most likely number of clusters is $K = 2$ according to the ΔK criterion, and LnPr(X|K) reached a plateau for the same K value (Supplementary Figure S3C). These two genetic clusters split western and eastern populations, with population DAVA located in the centre of the distribution showing a considerable degree of admixed ancestry (ca. 50%; Figures 2 and 3; Supplementary Figure S4B). Finally, analyses for *P. l. birandi* identify that the most likely number of clusters is $K = 2$ according to the ΔK criterion, but LnPr(X|K) reached a plateau at $K = 5$ (Supplementary Figure S3D). All populations split hierarchically into different genetic clusters from $K = 2$ to $K = 5$ with very limited signatures of genetic admixture (Figure 2; Supplementary Figure S4B). PCAs including all populations separate well the three taxa and the two lineages of *P. l. luschani* (Supplementary Figure S5), and independent PCAs for each subspecies split populations in line with the results from STRUCTURE (Supplementary Figure S5). SVDQUARTETS fully supported the monophyly of all subspecies (Figure 3). However, the phylogenetic relationships among taxa were not well resolved, suggesting post-divergence gene flow (see section Testing alternative models of divergence). In line with patterns of genetic admixture revealed by STRUCTURE analyses, relationships among some geographically proximate populations from the same subspecies were not well resolved (Figure 3).

Landscape genetic analyses

Genetic differentiation (F_{ST}) between populations (Supplementary Table S1) is positively correlated with both geographical distance ($r = .629$, $p < .001$) and topographic distance ($r = .629$, $p < .001$) in analyses including all populations, with both matrices providing a virtually identical fit to the data. Analyses only considering comparisons between populations within the same subspecies also reveal a strong correlation between genetic differentiation and both geographical distance ($r = .537$, $p < .001$; Figure 4) and topographic distance ($r = .567$, $p < .001$). In this case, topographic distance provides a better fit to the data, and it is the only variable that remains significant after controlling for each other in partial Mantel tests (geographical distance: $r = -.272$, $p = .907$; topographic distance: $r = .342$, $p = .047$). However, genetic differentiation is not significantly correlated with geographical distance ($r = -.018$, $p = .554$; Figure 4) or topographic distance ($r = -.025$, $p = .583$) in analyses only considering comparisons involving populations from different subspecies (Figure 4).

Testing alternative models of divergence

The scenario best explaining the formation of the three subspecies of *P. luschani* is one that models divergence in strict isolation followed by secondary contact and gene flow during a limited period of time (Model B1; Table 2; Figure 5); the rest of the tested models received comparatively much lower statistical support ($\Delta AIC > 12$; Table 2). Considering a 1-year generation time, the split of the sister taxa *P. l. chobanovi* and *P. l. luschani* is estimated to have taken place during the Middle Pleistocene (ca. 0.67 Ma; Chibanian age), shortly after the divergence of their most recent common ancestor from *P. l. birandi* (ca. 0.72 Ma) (Table 3; Figure 5). Post-divergence gene flow is inferred to have taken place during the last glacial period (44–32 ka ago), and migration rates per generation (m) among subspecies are estimated to be consistently low ($<2 \times 10^{-6}$; Table 3; Figure 5).

Inference of past demographic history

STAIRWAY PLOT analyses reveal that the three putative subspecies within the taxon *P. luschani* have experienced parallel changes of N_e through time, undergoing expansions during the last glacial period followed by severe demographic declines starting at the onset of the Holocene (Figure 2D).

Discussion

Elucidating the processes underlying microgeographic speciation is of paramount importance to understanding the extraordinary diversity of some organism groups and the high levels of local endemism characterizing biodiversity hotspots. Our study supports recent microgeographic speciation (<1 Ma) within the species complex *P. luschani*, pointing to population isolation and quick evolution of total or partial reproductive isolation as key drivers of the extraordinary diversity of this speciose genus (Borissov et al., 2023; Cigliano et al., 2023). Genomic data also revealed the presence of two sympatric cryptic sister lineages, which indicates hidden diversity within the species flock and reinforces the notion of fast diversification over small spatiotemporal scales.

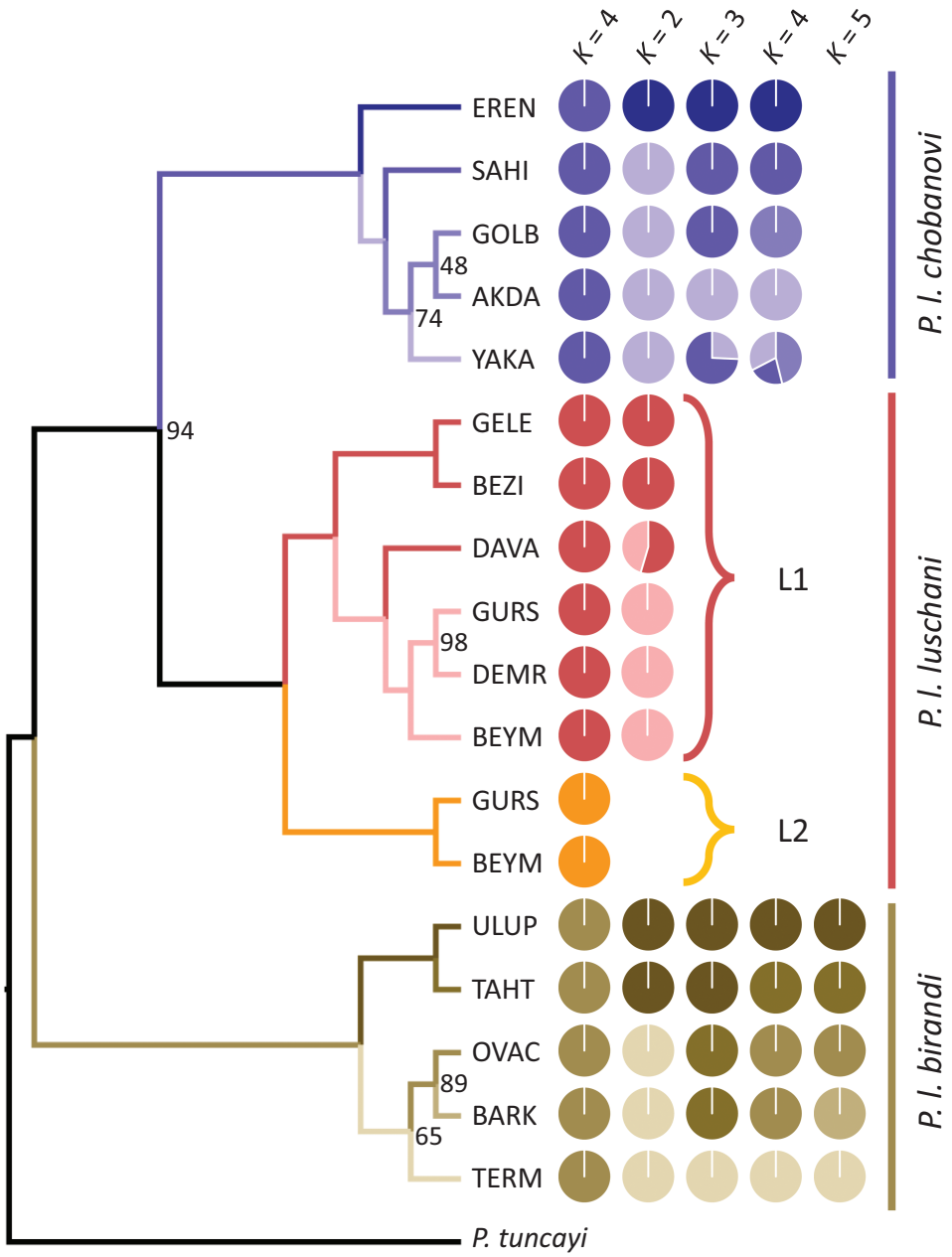

Figure 3. Phylogenetic relationships among populations of the three subspecies of *Poecilimon luschani* as inferred by SVDQUARTETS and their genetic assignments based on STRUCTURE (pie charts) for the different *K*, genetic clusters. The two sympatric cryptic lineages of *P. l. luschani* (L1 and L2) were analysed separately. Nodes have a bootstrap support of 100% unless otherwise indicated on the tree. Hierarchical STRUCTURE analyses were run for all populations of the three subspecies jointly (6,611 SNPs; pie charts on the left) and independently for populations of each subspecies (*P. l. chobanovi*: 10,419 SNPs; *P. l. luschani*: 18,392 SNPs; *P. l. birandi*: 17,369 SNPs; rest of the pie charts of $K = 2$ through $K = 5$). Pie charts show the results of STRUCTURE for *K*-values between $K = 2$ and the value of *K* at which the log probability of the data (LnPr(X|*K*)) reached a plateau for each dataset (see Supplementary Figure S3). Results from $K = 2$ to $K = 5$ are presented in Supplementary Figure S4. Population codes as described in Table 1.

Diversification of the species group

Phylogenomic reconstructions including the eight taxa within the species group *P. luschani* (Boztepe et al., 2013; Cigliano et al., 2023; Table 1) revealed that sister clades and taxa are distributed in adjacent regions, supporting the prime geographic dimension of speciation in the complex (Figure 1). The estimated timing of diversification indicates the Pleistocene origin of the group, with divergence times ranging between 1.08 Ma for the two main subclades to 0.28 Ma for the split of the two cryptic lineages (L1 and L2) within the taxon *P. l. luschani* (Figure 1). These estimates are in good agreement with those obtained based on mtDNA and a combined matrix of a few nuclear and mtDNA markers, which placed the origin of the group ca. 1.4–1.6 Ma (Borissov et al., 2023; Kaya et al., 2015). Although the diversification of the genus *Poecilimon* dates back to the end of the Miocene (ca. 9 Ma), and is likely associated with ancient geological events in the Mediterranean region such as the Messinian Salinity Crisis and changes in the configuration of Aegean-Anatolian landmasses, Pleistocene splits in terminals of most clades seem to be largely responsible for the high number of narrow endemic taxa characterizing this radiation (Borissov

et al., 2023). This divergence history, together with the allopatric distribution of most lineages, points to a predominant role of population isolation in the diversification of most recent clades, which was likely facilitated by the interplay between the complex topography of the region and distributional shifts (i.e., range contractions–expansions) linked to Pleistocene climatic oscillations (e.g., Kaya et al., 2015; Ortego & Knowles, 2022).

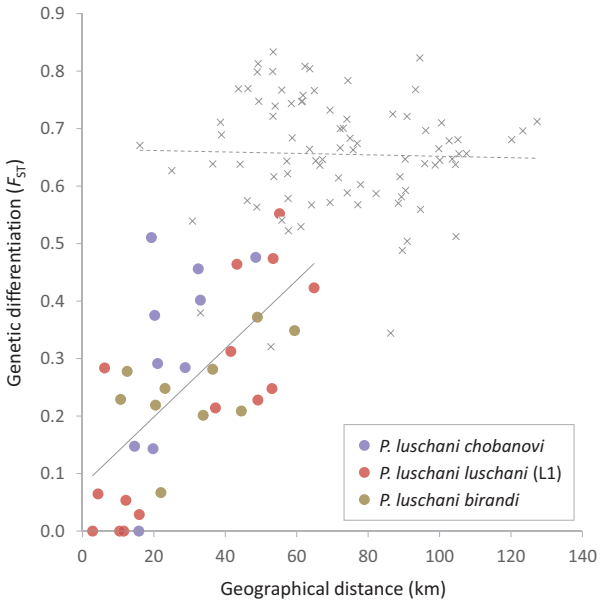

Figure 4. Relationship between genetic differentiation (F_{ST}) and geographical distance in comparisons within subspecies (coloured dots, solid regression line) or across subspecies (crosses, dashed regression line) of *Poecilimon luschani*. Analyses only considered lineage L1 for the subspecies *P. l. luschani*.

Evolutionary distinctiveness of lineages

Phylogenomic analyses confirmed that all lineages of *P. luschani* originated from a common ancestor during the Pleistocene (Figure 1), supporting recent diversification (<1 Ma) within a small geographical area (ca. 120 × 80 km) in the Teke Peninsula (Figure 2). Our genomic data support the genetic cohesiveness and monophyly of the different subspecific taxa within *P. luschani*, which could not be resolved in a previous mtDNA-based study likely due to recent divergence and incomplete lineage sorting (Boztepe et al., 2013; Kaya et al., 2015). Accordingly, Bayesian clustering analyses revealed that populations of each putative subspecies separate into different genetic clusters, present abrupt genetic discontinuities coinciding with contemporary range boundaries, and show no evidence of genetic admixture either between nearby populations at the geographical limits of subspecies distributions (i.e., putative areas of historical secondary contact) or between the two sympatric cryptic sister lineages (L1 and L2) within *P. l. luschani* (Figure 2). The genetic cohesiveness among populations of each subspecies and sharp genetic discontinuities across their respective range boundaries are further supported by landscape genetic analyses, considering the role of topography and geographical distances in structuring genetic variation within the complex. These analyses show that genetic differentiation between pairs of populations from the same putative subspecies is significantly correlated with topographical-weighted distances, whereas comparisons involving populations of the different taxa do not show any significant correlation with either geographical or topographic distances (Figure 4). Along the same line, although clustering analyses indicate a marked genetic fragmentation, they also provide evidence of admixture and ongoing gene flow among certain nearby populations from the same taxon (e.g., YAKA in *P. l. chobanovi* and DAVA in *P. l. luschani*; Figure 2C). Thus, genomic data support that con(sub)specific populations are at migration-drift equilibrium and exchange gene flow across the landscape at a rate that is shaped by the spatial configuration of corridors and barriers to dispersal, in line with

Table 2. Alternative models of divergence for the three subspecies within the taxon *Poecilimon luschani* tested using FASTSIMCOAL2, with the best-supported scenario highlighted in bold (see Figure 5). Models are illustrated in Supplementary Figure S1 and include scenarios of divergence in strict isolation (Model A), divergence in strict isolation followed by secondary contact and gene flow during a limited period of time (Models B1–B3), and isolation-with-migration followed by interruption of gene flow (Models C1–C7). Models B and C considered alternative gene flow scenarios involving different contemporary and/or ancestral populations, as illustrated in Supplementary Figure S1. The site frequency spectrum used for FASTSIMCOAL2 analyses contained 1,931 variable SNPs.

Model	lnL	*k*	AIC	ΔAIC	ω*i*
A	−3,096.42	6	6,204.84	72.91	0.00
B1	**−3,055.96**	**10**	**6,131.93**	**0.00**	**1.00**
B2	−3,076.43	9	6,170.87	38.94	0.00
B3	−3,078.79	9	6,175.59	43.66	0.00
C1	−3,063.01	10	6,146.02	14.10	0.00
C2	−3,079.67	9	6,177.33	45.40	0.00
C3	−3,081.99	9	6,181.98	50.05	0.00
C4	−3,096.34	8	6,208.67	76.75	0.00
C5	−3,063.14	9	6,144.28	12.35	0.00
C6	−3,079.33	8	6,174.65	42.72	0.00
C7	−3,082.02	8	6,180.03	48.11	0.00

Note. ΔAIC = difference in AIC value from that of the strongest model; AIC = Akaike's information criterion value; *k* = number of parameters in the model; lnL = maximum likelihood value of the model; ω_i = AIC weight.

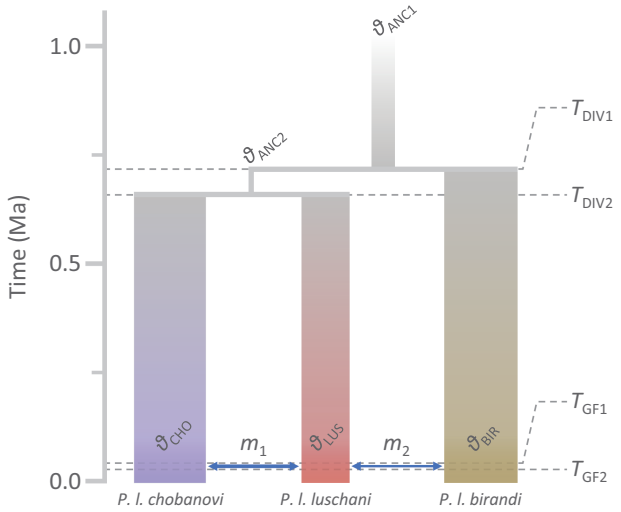

Figure 5. Schematic of the best-supported model (Model B1) of divergence for the three currently recognized subspecies within the taxon *Poecilimon luschani* as inferred from coalescent simulations with FASTSIMCOAL2. Parameters include mutation-scaled ancestral (θ_{ANC1}, θ_{ANC2}) and contemporary (θ_{CHO}, θ_{LUS}, θ_{BIR}) effective population sizes, migration rates per generation (m_1, m_2), timing of divergence (T_{DIV1}, T_{DIV2}), and timing (beginning and end) of gene flow (T_{GF1}, T_{GF2}). Point estimates yielded by FASTSIMCOAL2 were used to scale the different time events (T, left axis), effective population sizes (θ, proportional to branch width), and migration rates per generation (m, proportional to arrow thickness). Demographic parameter values and confidence intervals are detailed in Table 3. Contemporary effective population size of the *P. l. chobanovi* (θ_{CHO}) was calculated from its levels of nucleotide diversity (π) and fixed in FASTSIMCOAL2 analyses to enable the estimation of all other parameters (see the section Testing alternative models of divergence for further details).

Table 3. Parameters inferred from coalescent simulations with FASTSIMCOAL2 under the most likely scenario of divergence (Model B1; Figure 5) for the three subspecies within the taxon *Poecilimon luschani*. Shown are point estimates and lower and upper 95% confidence intervals for each parameter, which include the mutation-scaled ancestral (θ_{ANC1}, θ_{ANC2}) and contemporary (θ_{CHO}, θ_{LUS}, θ_{BIR}) effective population sizes, the migration rates per generation (m_1, m_2), the timing of divergence (T_{DIV1}, T_{DIV2}), and the timing (beginning and end) of gene flow (T_{GF1}, T_{GF2}), with time given in units of generations (or years, with one generation per year). Parameters are illustrated in Figure 5. Contemporary effective population size of *P. l. chobanovi* (θ_{CHO}) was calculated from its levels of nucleotide diversity (π) and fixed in FASTSIMCOAL2 analyses to enable the estimation of all other parameters (see the Testing alternative models of divergence section for further details).

Parameter	Point estimate	Lower bound	Upper bound
θ_{ANC1}	237,877	198,288	218,570
θ_{ANC2}	52,639	82,419	102,900
θ_{CHO}	741,901	—	—
θ_{LUS}	500,337	485,425	498,314
θ_{BIR}	754,602	728,855	751,800
T_{DIV1}	724,491	741,090	767,208
T_{DIV2}	665,935	645,988	666,609
T_{GF1}	43,950	100,906	147,600
T_{GF2}	31,891	15,349	20,482
m_1	1.08×10^{-6}	6.54×10^{-7}	1.97×10^{-6}
m_2	5.62×10^{-7}	3.90×10^{-7}	1.35×10^{-6}

spatial patterns of genetic structure inferred for intraspecific populations of other Orthoptera inhabiting topographically complex landscapes (González-Serna et al., 2019; Noguerales et al., 2016; Tonzo et al., 2019). Altogether, our analyses support that the three taxa and the two cryptic lineages behave as independently evolving units that fulfil multiple contemporary species concepts (i.e., phylogenetic, genotypic cluster, and biological species concepts; De Queiroz, 2007), suggesting they merit to be elevated to a full-species status in future taxonomic revisions of the genus (e.g., Borissov et al., 2023; Boztepe et al., 2013; see also section Cryptic speciation in *Poecilimon*).

Cryptic speciation in *Poecilimon*

An intriguing finding was the discovery of two cryptic lineages within the putative taxon *P. l. luschani* (Figures 1 and 3). Phylogenomic reconstructions support that these lineages are sister, and Bayesian clustering analyses showed no evidence of genetic admixture despite being co-distributed (Figures 1–3), indicating that they are reproductively isolated or present strong barriers to gene flow (Dynesius & Jansson, 2014). Although three of the four criteria proposed for diagnosing sympatric speciation events are fulfilled—the two lineages are (a) sympatric, (b) sister, and (c) strongly reproductively isolated—we cannot categorically discard (d) a historic phase of geographical isolation at the onset of divergence (Coyne & Orr, 2004). Considering the complex topography of the region, the limited dispersal capacity of *Poecilimon*, the strong genetic fragmentation of most contemporary populations, and the lack of evidence for ecological/environmental specialization, the most plausible scenario is that the two cryptic lineages originated allopatrically and then came into sympatry after one of them (or the two) experienced range expansions (Graham et al., 2004; e.g., Ortego et al., 2021; Rasolonjatovo et al., 2020; see also section Drivers of microgeographic speciation). The asymmetric ranges of the two lineages—one of them (L2) exclusively present in two nearby localities at the easternmost portion of the distribution of *P. l. luschani*—might also be compatible with "budding" or "peripheral" speciation, in which a larger ranged progenitor (lineage L1) gave rise to a smaller ranged derivative lineage (lineage L2) (Anacker & Strauss, 2014; e.g., Kaya & Çıplak, 2016). Estimates of divergence time indicate that these two lineages likely split within the last 300 ka, further supporting the role of fast evolution of reproductive isolation and short speciation times in the formation of the large number of endemic taxa that populate the terminal Pleistocene splits in the phylogeny of *Poecilimon* (Borissov et al., 2023). The finding of two sister lineages with no evidence of genetic admixture in a natural contact zone suggests that all other older lineages probably show similar or stronger reproductive isolation (Coyne & Orr, 1989), which supports that all taxa within the complex and the two sister cryptic lineages within *P. luschani* represent independently evolving lineages and full-fledged species.

Drivers of microgeographic speciation

Different lines of evidence indicate that diversification of the species complex *P. luschani* at such a small geographical scale is the outcome of the concurrence of processes that have promoted lineage formation (i.e., population fragmentation) and contributed to their persistence through evolutionary time (i.e., quick evolution of reproductive isolation; <300

ka, see section Cryptic speciation in *Poecilimon*) (Dynesius & Jansson, 2014). Regarding lineage formation, the limited dispersal capacity of flightless *Poecilimon* and the complex topography of the region offer an ideal scenario for geographical diversification to take place, providing ample opportunities for igniting divergence under the classic model of allopatric speciation (Mayr, 1963). Accordingly, coalescent-based testing of alternative modes of speciation supports that divergence most likely took place in strict isolation, indicating that population fragmentation and vicariance played a primary role at the onset of species formation (Figure 5). The importance of topography and limited dispersal on population fragmentation is corroborated by clustering and spatially explicit landscape genetic analyses, which showed a marked genetic structure within each taxon at fine spatial scales (<10 km; Figure 2) and supported that genetic differentiation between populations is better explained by topographic complexity than by geographical distances (see section Landscape genetic analyses). The interplay between topography and range shifts driven by Pleistocene climatic fluctuations likely further contributed to population isolation through sufficient periods of time for initiating allopatric speciation (Carstens & Knowles, 2007; Knowles, 2000). In addition, reconstructions of changes in effective population size through time indicate that the three taxa experienced marked demographic fluctuations during the Late Quaternary (Figure 2C), which have likely contributed to population divergence in allopatric microrefugia during periods of demographic contractions (Stewart et al., 2010; e.g., Ortego & Knowles, 2022).

Although the above described processes point to the important role of population isolation at early stages of speciation, the persistence of newly generated lineages through evolutionary time (i.e., successful speciation) at such small spatiotemporal scales likely required the quick evolution of reproductive isolation. This is particularly important considering that the three subspecific taxa have geographically adjacent distributions and occupy similar habitats across wide elevational ranges, suggesting that environment- or ecology-based divergent selection has not played a role in either lineage formation or the subsequent maintenance of species boundaries (Papadopulos et al., 2011; Rundle & Nosil, 2005). The parallel demographic trajectories of the three taxa within the complex *P. luschani* indicate that they have responded in a similar way to past climate changes (Figure 2), supporting the notion of similar environmental requirements and niche conservatism in a non-adaptive allopatric radiation with limited phenotypic divergence (Graham et al., 2004; e.g., Kozak & Wiens, 2006). In line with the limited divergence in courtship behaviour in allopatric populations of other closely related species of Orthoptera (e.g., Jang & Gerhardt, 2006), calling song shows little variation within the *P. luschani* complex (Boztepe et al., 2013). This suggests that the evolution of reproductive isolation in the studied radiation is probably not linked to sexual selection (Panhuis et al., 2001; e.g., Ritchie, 1996). Considering the limited ecological and courtship behaviour divergence in the complex and the allopatric distribution of most taxa, the most parsimonious explanation is that speciation is the outcome of the progressive accumulation of reproductive isolation (e.g., genetic incompatibilities and/or divergence in internal genitalia resulted from genetic drift; Coyne & Orr, 1989; Langerhans et al., 2016; Mayr, 1963; Presgraves, 2010) as a by-product of separate evolutionary histories during periods of geographic isolation rather than a consequence of selection or adaptive processes (Mayr, 1963; e.g., Hagberg et al., 2022). Future experimental hybridization attempts in the laboratory might help to determine the extent of reproductive isolation in the complex and elucidate the presence of pre- and postzygotic barriers to interspecific gene flow (e.g., Saldamando et al., 2005).

Although a quick evolution of reproductive isolation was likely instrumental to avoid lineage fusion and speciation reversal, coalescent analyses indicate that the three taxa have exchanged gene flow coinciding with demographic expansions during glacial periods (Figure 5). The fact that contemporary populations of each lineage show strong genetic cohesiveness and the timing of their formation (>300 ka) largely predates the last episode of gene flow (<15 ka) suggests that lineages are not ephemeral and semi-permeable species boundaries have not compromised their evolutionary and genetic distinctiveness through time (Dynesius & Jansson, 2014; e.g., Ortego & Knowles, 2022). Albeit speculative, one possibility is that limited periods of secondary contact during demographic expansions might have even potentially contributed to the progressive completion of speciation via reinforcement of reproductive isolation (i.e., selection against hybrids; Servedio & Noor, 2003).

Conclusions

Our study supports the role of fine-scale allopatric divergence and quick evolution of total or partial reproductive isolation on microgeographic speciation, which can explain the high number of narrow endemic species in the Mediterranean region and other biodiversity hotspots. Our analyses suggest that speciation at such small spatiotemporal scales is probably the outcome of the interplay of multiple factors that contribute to both the formation and persistence of independently evolving lineages (Dynesius & Jansson, 2014). Regarding lineage formation, high topographic complexity, limited dispersal capacity, and demographic expansions/contractions fuelled by Pleistocene climatic oscillations have likely contributed to population isolation and lineage diversification. Although most lineages originated by such processes are probably ephemeral and likely merge after secondary contact (e.g., Maier et al., 2019), our data suggest that short speciation times (<300 ka) seem to frequently lead to the successful formation of independently evolving entities. Steep environmental gradients might ultimately contribute to species persistence in microclimatic refugia and reduce their chances of extinction through time (Nieto Feliner, 2011; Tzedakis, 2009). Although the specific processes underlying the quick evolution of reproductive isolation remain to be studied, different lines of evidence suggest that speciation could have been driven by the incidental accumulation of reproductive incompatibilities during periods of isolation rather than as a direct outcome or a by-product of natural (e.g., local adaptation) or sexual (e.g., divergence in courtship behaviour) selection. With a great majority of invertebrates yet to be analysed genomically, our study anticipates further discovery of a high number of microendemic cryptic species in the Mediterranean biodiversity hotspot.

Supplementary material

Supplementary material is available at *Journal of Evolutionary Biology* online.

Data availability

Raw Illumina reads have been deposited at the NCBI Sequence Read Archive (SRA) under BioProject PRJNA976820. Input files for all analyses (STACKS, PYRAD, BPP, STRUCTURE, PCAs, SVDQUARTETS, ARLEQUIN, FASTSIMCOAL2, and STAIRWAY PLOT) are available for download on Figshare (https://doi.org/10.6084/m9.figshare.23244212).

Author contributions

Joaquín Ortego (Conceptualization [equal], Data curation [equal], Formal analysis [lead], Investigation [equal], Methodology [equal], Validation [equal], Visualization [equal], Writing—original draft [lead], Writing—review & editing [lead]), Sarp Kaya (Conceptualization [equal], Data curation [equal], Formal analysis [supporting], Investigation [equal], Methodology [supporting], Validation [equal], Visualization [equal], Writing—review & editing [supporting]), Battal Ciplak (Conceptualization [equal], Data curation [equal], Funding acquisition [equal], Investigation [equal], Project administration [equal], Validation [equal], Visualization [equal], Writing—review & editing [supporting]), and L. Lacey Knowles (Conceptualization [equal], Data curation [equal], Formal analysis [supporting], Funding acquisition [equal], Investigation [equal], Methodology [equal], Project administration [equal], Supervision [lead], Validation [equal], Visualization [equal], Writing—original draft [supporting], Writing—review & editing [supporting])

Funding

Specimens used in this study were obtained via two grants to B.Ç., one funded by Akdeniz University (grant no. 2010.02.0121.028) and the other funded by the Scientific and Technical Research Council of Turkey (TUBITAK, grant no. 210T169). This work was supported by grant PID2021-123298NB-I00 funded by MCIN/AEI/10.13039/501100011033/FEDER, UE and grant TED2021-129328B-I00 funded by MCIN/AEI/10.13039/501100011033 and European Union NextGenerationEU/PRTR.

Acknowledgments

We thank Dragan Chobanov for providing samples of *Poecilimon orbelicus* from Bulgaria, Zehra Boztepe for participating in field studies, Sergio Pereira (the Centre for Applied Genomics) for Illumina sequencing, and Mark Ravinet and two anonymous reviewers for their constructive and valuable comments on an earlier version of the manuscript. We also thank Centro de Supercomputación de Galicia (CESGA) and Doñana's Singular Scientific-Technical Infrastructure (ICTS-RBD) for access to computer resources.

Conflicts of interest

The authors have no conflicts of interest to declare.

References

Anacker, B. L., & Strauss, S. Y. (2014). The geography and ecology of plant speciation: Range overlap and niche divergence in sister species. *Proceedings of the Royal Society B: Biological Sciences*, *281*(1778), 20132980. https://doi.org/10.1098/rspb.2013.2980

Bonnet, E., & Van de Peer, Y. (2002). ZT: A software tool for simple and partial Mantel tests. *Journal of Statistical Software*, *7*(10), 1–12.

Borissov, S. B., Heller, K. -G., Çıplak, B., & Chobanov, D. P. (2023). Origin, evolution and systematics of the genus *Poecilimon* (Orthoptera: Tettigoniidae)—An outburst of diversification in the Aegean area. *Systematic Entomology*, *48*(1), 198–220. https://doi.org/10.1111/syen.12580

Boztepe, Z., Kaya, S., & Çıplak, B. (2013). Integrated systematics of the *Poecilimon luschani* species group (Orthoptera, Tettigoniidae): Radiation as a chain of populations in a small heterogeneous area. *Zoological Journal of the Linnean Society*, *169*(1), 43–69. https://doi.org/10.1111/zoj.12058

Bradford, J., & Jaffre, T. (2004). Plant species microendemism and conservation of montane maquis in New Caledonia: Two new species of *Pancheria* (Cunoniaceae) from the Roche Ouaieme. *Biodiversity and Conservation*, *13*(12), 2253–2274. https://doi.org/10.1023/b:bioc.0000047901.33761.3c

Carstens, B. C., & Knowles, L. L. (2007). Shifting distributions and speciation: Species divergence during rapid climate change. *Molecular Ecology*, *16*(3), 619–627. https://doi.org/10.1111/j.1365-294X.2006.03167.x

Catchen, J., Hohenlohe, P. A., Bassham, S., Amores, A., & Cresko, W. A. (2013). Stacks: An analysis tool set for population genomics. *Molecular Ecology*, *22*(11), 3124–3140. https://doi.org/10.1111/mec.12354

Cigliano, M. M., Braun, H., Eades, D. C., & Otte, D. (2023). *Orthoptera species file* (OSF). http://orthoptera.speciesfile.org

Çıplak, B. (2003). Distribution of *Tettigoniinae* (Orthoptera, Tettigoniidae) bush-crickets in Turkey: The importance of the Anatolian Taurus Mountains in biodiversity and implications for conservation. *Biodiversity and Conservation*, *12*(1), 47–64.

Cowling, R. M., & Pressey, R. L. (2001). Rapid plant diversification: Planning for an evolutionary future. *Proceedings of the National Academy of Sciences of the United States of America*, *98*(10), 5452–5457. https://doi.org/10.1073/pnas.101093498

Coyne, J. A., & Orr, H. A. (1989). Patterns of speciation in *Drosophila*. *Evolution*, *43*(2), 362–381. https://doi.org/10.1111/j.1558-5646.1989.tb04233.x

Coyne, J. A., & Orr, H. A. (2004). *Speciation*. Sinauer Associates.

De Queiroz, K. (2007). Species concepts and species delimitation. *Systematic Biology*, *56*(6), 879–886. https://doi.org/10.1080/10635150701701083

Dynesius, M., & Jansson, R. (2014). Persistence of within-species lineages: A neglected control of speciation rates. *Evolution*, *68*(4), 923–934. https://doi.org/10.1111/evo.12316

Eaton, D. A. R. (2014). PyRAD: Assembly of *de novo* RADseq loci for phylogenetic analyses. *Bioinformatics*, *30*(13), 1844–1849. https://doi.org/10.1093/bioinformatics/btu121

Evanno, G., Regnaut, S., & Goudet, J. (2005). Detecting the number of clusters of individuals using the software STRUCTURE: A simulation study. *Molecular Ecology*, *14*(8), 2611–2620. https://doi.org/10.1111/j.1365-294X.2005.02553.x

Excoffier, L., Dupanloup, I., Huerta-Sanchez, E., Sousa, V. C., & Foll, M. (2013). Robust demographic inference from genomic and SNP data. *PLoS Genetics*, *9*(10), e1003905. https://doi.org/10.1371/journal.pgen.1003905

Excoffier, L., & Lischer, H. E. L. (2010). ARLEQUIN suite ver 35: A new series of programs to perform population genetics analyses under Linux and Windows. *Molecular Ecology Resources*, *10*(3), 564–567. https://doi.org/10.1111/j.1755-0998.2010.02847.x

Flouri, T., Jiao, X. Y., Rannala, B., & Yang, Z. H. (2018). Species tree inference with BPP using genomic sequences and the multispecies coalescent. *Molecular Biology and Evolution*, *35*(10), 2585–2593.

Goldblatt, P., & Manning, J. C. (2002). Plant diversity of the Cape Region of southern Africa. *Annals of the Missouri Botanical Garden*, *89*(2), 281–302. https://doi.org/10.2307/3298566

Gómez, A., & Lunt, D. H. (2007). Refugia within refugia: Patterns of phylogeographic concordance in the Iberian Peninsula. In S. Weiss & N. Ferrand (Eds.), *Phylogeography of southern European refugia* (pp. 155–188). Springer Verlag.

González-Serna, M. J., Cordero, P. J., & Ortego, J. (2018). Using high-throughput sequencing to investigate the factors structuring genomic variation of a Mediterranean grasshopper of great conservation concern. *Scientific Reports*, *8*(1), 13436. https://doi.org/10.1038/s41598-018-31775-x

González-Serna, M. J., Cordero, P. J., & Ortego, J. (2019). Spatiotemporally explicit demographic modelling supports a joint effect of historical barriers to dispersal and contemporary landscape composition on structuring genomic variation in a red-listed grasshopper. *Molecular Ecology*, *28*(9), 2155–2172. https://doi.org/10.1111/mec.15086

Graham, C. H., Ron, S. R., Santos, J. C., Schneider, C. J., & Moritz, C. (2004). Integrating phylogenetics and environmental niche models to explore speciation mechanisms in dendrobatid frogs. *Evolution*, *58*(8), 1781–1793. https://doi.org/10.1111/j.0014-3820.2004.tb00461.x

Grandcolas, P., Nattier, R., & Trewick, S. (2014). Relict species: A relict concept? *Trends in Ecology & Evolution*, *29*(12), 655–663. https://doi.org/10.1016/j.tree.2014.10.002

Hagberg, L., Celemin, E., Irisarri, I., Hawlitschek, O., Bella, J. L., Mott, T., & Pereira, R. J. (2022). Extensive introgression at late stages of species formation: Insights from grasshopper hybrid zones. *Molecular Ecology*, *31*(8), 2384–2399. https://doi.org/10.1111/mec.16406

Huang, J. P., Hill, J. G., Ortego, J., & Knowles, L. L. (2020). Paraphyletic species no more - genomic data resolve a Pleistocene radiation and validate morphological species of the *Melanoplus scudderi* complex (Insecta: Orthoptera). *Systematic Entomology*, *45*(3), 594–605.

Janes, J. K., Miller, J. M., Dupuis, J. R., Malenfant, R. M., Gorrell, J. C., Cullingham, C. I., & Andrew, R. L. (2017). The *K*=2 conundrum. *Molecular Ecology*, *26*(14), 3594–3602. https://doi.org/10.1111/mec.14187

Jang, Y., & Gerhardt, H. C. (2006). Divergence in the calling songs between sympatric and allopatric populations of the southern wood cricket *Gryllus fultoni* (Orthoptera: Gryllidae). *Journal of Evolutionary Biology*, *19*(2), 459–472. https://doi.org/10.1111/j.1420-9101.2005.01014.x

Jombart, T. (2008). Adegenet: A R package for the multivariate analysis of genetic markers. *Bioinformatics*, *24*(11), 1403–1405. https://doi.org/10.1093/bioinformatics/btn129

Kaya, S., Boztepe, Z., & Çıplak, B. (2015). Phylogeography of the *Poecilimon luschani* species group (Orthoptera, Tettigoniidae): A radiation strictly correlated with climatic transitions in the Pleistocene. *Zoological Journal of the Linnean Society*, *173*(1), 1–21.

Kaya, S., & Çıplak, B. (2016). Budding speciation via peripheral isolation: The *Psorodonotus venosus* (Orthoptera, Tettigoniidae) species group example. *Zoologica Scripta*, *45*(5), 521–537. https://doi.org/10.1111/zsc.12174

Kaya, S., Gunduz, I., & Çıplak, B. (2012). Estimating effects of global warming from past range changes for cold demanding refugial taxa: A case study on South-west Anatolian species *Poecilimon birandi*. *Biologia*, *67*(6), 1152–1164. https://doi.org/10.2478/s11756-012-0111-0

Keightley, P. D., Ness, R. W., Halligan, D. L., & Haddrill, P. R. (2014). Estimation of the spontaneous mutation rate per nucleotide site in a *Drosophila melanogaster* full-sib family. *Genetics*, *196*(1), 313–320. https://doi.org/10.1534/genetics.113.158758

Keightley, P. D., Pinharanda, A., Ness, R. W., Simpson, F., Dasmahapatra, K. K., Mallet, J., & Jiggins, C. D. (2015). Estimation of the spontaneous mutation rate in *Heliconius melpomene*. *Molecular Biology and Evolution*, *32*(1), 239–243.

Knowles, L. L. (2000). Tests of Pleistocene speciation in montane grasshoppers (genus *Melanoplus*) from the sky islands of western North America. *Evolution*, *54*(4), 1337–1348. https://doi.org/10.1111/j.0014-3820.2000.tb00566.x

Kozak, K. H., & Wiens, J. J. (2006). Does niche conservatism promote speciation? A case study in North American salamanders. *Evolution*, *60*(12), 2604–2621.

Langerhans, R. B., Anderson, C. M., & Heinen-Kay, J. L. (2016). Causes and consequences of genital evolution. *Integrative and Comparative Biology*, *56*(4), 741–751. https://doi.org/10.1093/icb/icw101

Levin, D. A. (1993). Local speciation in plants: The rule not the exception. *Systematic Botany*, *18*(2), 197–208. https://doi.org/10.2307/2419397

Li, J. C., Huang, J. P., Sukumaran, J., & Knowles, L. L. (2018). Microevolutionary processes impact macroevolutionary patterns. *BMC Evolutionary Biology*, *18*, 123.

Liu, X. M., & Fu, Y. X. (2020). Stairway Plot 2: Demographic history inference with folded SNP frequency spectra. *Genome Biology*, *21*(1), 280.

Maier, P. A., Vandergast, A. G., Ostoja, S. M., Aguilar, A., & Bohonak, A. J. (2019). Pleistocene glacial cycles drove lineage diversification and fusion in the Yosemite toad (*Anaxyrus canorus*). *Evolution*, *73*(12), 2476–2496. https://doi.org/10.1111/evo.13868

Massatti, R., & Knowles, L. L. (2014). Microhabitat differences impact phylogeographic concordance of codistributed species: Genomic evidence in montane sedges (*Carex* L) from the Rocky Mountains. *Evolution*, *68*(10), 2833–2846. https://doi.org/10.1111/evo.12491

Mayr, E. (1963). *Animal species and evolution*. The Belknap Press of Harvard University Press.

Medail, F., & Quezel, P. (1997). Hot-spots analysis for conservation of plant biodiversity in the Mediterranean basin. *Annals of the Missouri Botanical Garden*, *84*(1), 112–127. https://doi.org/10.2307/2399957

Moreau, C. S., & Bell, C. D. (2013). Testing the museum versus cradle tropical biological diversity hypothesis: Phylogeny, diversification, and ancestral biogeographic range evolution of the ants. *Evolution*, *67*(8), 2240–2257. https://doi.org/10.1111/evo.12105

Moritz, C. (2002). Strategies to protect biological diversity and the evolutionary processes that sustain it. *Systematic Biology*, *51*(2), 238–254. https://doi.org/10.1080/10635150252899752

Musher, L. J., Giakoumis, M., Albert, J., Del-Rio, G., Rego, M., Thom, G., & Cracraft, J. (2022). River network rearrangements promote speciation in lowland Amazonian birds. *Science Advances*, *8*(14), eabn1099.

Myers, N., Mittermeier, R. A., Mittermeier, C. G., da Fonseca, G. A. B., & Kent, J. (2000). Biodiversity hotspots for conservation priorities. *Nature*, *403*(6772), 853–858. https://doi.org/10.1038/35002501

Nieto Feliner, G. (2011). Southern European glacial refugia: A tale of tales. *Taxon*, *60*(2), 365–372. https://doi.org/10.1002/tax.602007

Nieto Feliner, G. (2014). Patterns and processes in plant phylogeography in the Mediterranean Basin: A review. *Perspectives in Plant Ecology Evolution and Systematics*, *16*(5), 265–278. https://doi.org/10.1016/j.ppees.2014.07.002

Noguerales, V., Cordero, P. J., Knowles, L. L., & Ortego, J. (2021). Genomic insights into the origin of trans-Mediterranean disjunct distributions. *Journal of Biogeography*, *48*(2), 440–452.

Noguerales, V., Cordero, P. J., & Ortego, J. (2016). Hierarchical genetic structure shaped by topography in a narrow-endemic montane grasshopper. *BMC Evolutionary Biology*, *16*, 96. https://doi.org/10.1186/s12862-016-0663-7

Ortego, J., González-Serna, M. J., Noguerales, V., & Cordero, P. J. (2022). Genomic inferences in a thermophilous grasshopper provide insights into the biogeographic connections between northern African and southern European arid-dwelling faunas. *Journal of Biogeography*, *49*(9), 1696–1710.

Ortego, J., Gugger, P. F., & Sork, V. L. (2018). Genomic data reveal cryptic lineage diversification and introgression in Californian golden cup oaks (section *Protobalanus*). *The New Phytologist*, *218*(2), 804–818. https://doi.org/10.1111/nph.14951

Ortego, J., Gutiérrez-Rodríguez, J., & Noguerales, V. (2021). Demographic consequences of dispersal-related trait shift in two recently diverged taxa of montane grasshoppers. *Evolution*, *75*(8), 1998–2013. https://doi.org/10.1111/evo.14205

Ortego, J., & Knowles, L. L. (2022). Geographical isolation versus dispersal: Relictual alpine grasshoppers support a model of interglacial

diversification with limited hybridization. *Molecular Ecology*, *31*(1), 296–312. https://doi.org/10.1111/mec.16225

Panhuis, T. M., Butlin, R., Zuk, M., & Tregenza, T. (2001). Sexual selection and speciation. *Trends in Ecology & Evolution*, *16*(7), 364–371. https://doi.org/10.1016/s0169-5347(01)02160-7

Papadopulos, A. S. T., Baker, W. J., Crayn, D., Butlin, R. K., Kynast, R. G., Hutton, I., & Savolainen, V. (2011). Speciation with gene flow on Lord Howe Island. *Proceedings of the National Academy of Sciences of the United States of America*, *108*(32), 13188–13193. https://doi.org/10.1073/pnas.1106085108

Peterson, B. K., Weber, J. N., Kay, E. H., Fisher, H. S., & Hoekstra, H. E. (2012). Double digest RADseq: An inexpensive method for *de novo* SNP discovery and genotyping in model and non-model species. *PLoS One*, *7*(5), e37135. https://doi.org/10.1371/journal.pone.0037135

Presgraves, D. C. (2010). The molecular evolutionary basis of species formation. *Nature Reviews Genetics*, *11*(3), 175–180. https://doi.org/10.1038/nrg2718

Pritchard, J. K., Stephens, M., & Donnelly, P. (2000). Inference of population structure using multilocus genotype data. *Genetics*, *155*(2), 945–959. https://doi.org/10.1093/genetics/155.2.945

R Core Team. (2023). *r: A language and environment for statistical computing*. R Foundation for Statistical Computing. https://www.R-project.org/

Rasolonjatovo, S. M., Scherz, M. D., Hutter, C. R., Glaw, F., Rakotoarison, A., Razafindraibe, J. H., Goodman, S. M., Raselimanana, A. P., Vences, M., & Vences, M. (2020). Sympatric lineages in the *Mantidactylus ambreensis* complex of Malagasy frogs originated allopatrically rather than by in-situ speciation. *Molecular Phylogenetics and Evolution*, *144*, 106700. https://doi.org/10.1016/j.ympev.2019.106700

Ritchie, M. G. (1996). The shape of female mating preferences. *Proceedings of the National Academy of Sciences of the United States of America*, *93*(25), 14628–14631. https://doi.org/10.1073/pnas.93.25.14628

Rundle, H. D., & Nosil, P. (2005). Ecological speciation. *Ecology Letters*, *8*(3), 336–352. https://doi.org/10.1111/j.1461-0248.2004.00715.x

Saldamando, C. I., Tatsuta, H., & Butlin, R. K. (2005). Hybrids between *Chorthippus brunneus* and *C. jacobsi* (Orthoptera: Acrididae) do not show endogenous postzygotic isolation. *Biological Journal of the Linnean Society*, *84*(2), 195–203. https://doi.org/10.1111/j.1095-8312.2005.000424.x

Servedio, M. R., & Noor, M. A. F. (2003). The role of reinforcement in speciation: Theory and data. *Annual Review of Ecology, Evolution, and Systematics*, *34*, 339–364.

Singhal, S., Colli, G. R., Grundler, M. R., Costa, G. C., Prates, I., & Rabosky, D. L. (2022). No link between population isolation and speciation rate in squamate reptiles. *Proceedings of the National Academy of Sciences of the United States of America*, *119*(4), e2113388119. https://doi.org/10.1073/pnas.2113388119

Stebbins, G. L. (1974). *Flowering plants: Evolution above the species level*. The Belknap Press of Harvard University Press.

Steinbauer, M. J., Irl, S. D. H., & Beierkuhnlein, C. (2013). Elevation-driven ecological isolation promotes-diversification on Mediterranean islands. *Acta Oecologica*, *47*, 52–56.

Stewart, J. R., Lister, A. M., Barnes, I., & Dalen, L. (2010). Refugia revisited: Individualistic responses of species in space and time. *Proceedings of the Royal Society B: Biological Sciences*, *277*(1682), 661–671. https://doi.org/10.1098/rspb.2009.1272

Swofford, D. L. (2002). *PAUP*. Phylogenetic analysis using parsimony (* and other methods). Version 4*. Sinauer Associates.

Tonzo, V., Papadopoulou, A., & Ortego, J. (2019). Genomic data reveal deep genetic structure but no support for current taxonomic designation in a grasshopper species complex. *Molecular Ecology*, *28*(17), 3869–3886. https://doi.org/10.1111/mec.15189

Tzedakis, P. C. (2009). Museums and cradles of Mediterranean biodiversity. *Journal of Biogeography*, *36*(6), 1033–1034. https://doi.org/10.1111/j.1365-2699.2009.02123.x

Wang, I. J. (2020). Topographic path analysis for modelling dispersal and functional connectivity: Calculating topographic distances using the topoDistance r package. *Methods in Ecology and Evolution*, *11*(2), 265–272. https://doi.org/10.1111/2041-210x.13317

Wilmé, L., Goodman, S. M., & Ganzhorn, J. U. (2006). Biogeographic evolution of Madagascar's microendemic biota. *Science*, *312*(5776), 1063–1065. https://doi.org/10.1126/science.1122806